



# Flood risk assessment due to cyclone induced dike breaching on coastal areas of Bangladesh

Md Feroz Islam<sup>1</sup>, Biswa Bhattacharya<sup>2</sup>, Ioana Popescu<sup>2</sup>

<sup>1</sup>Copernicus Institute, Department of Environmental Sciences, Utrecht University, Utrecht, 3584 CB, the Netherlands

5 <sup>2</sup>IHE Delft Institute for Water Education, Delft, 2611 AX, the Netherlands

*Correspondence to:* M. F. Islam (m.f.islam@uu.nl)

**Abstract.** Bangladesh, one of the most disaster-prone countries in the world, has a dynamic delta with 123 polders protected by earthen dikes. Cyclone induced storm surges cause severe damages to these polders by overtopping and breaching the dikes. Nineteen major tropical storms hit the coast in last 50 years and storm intensity is predicted to increase due to climate change. The present paper presents an investigation of the inundation pattern in a protected area behind dikes due to floods caused by storm surges and identifies possible critical locations of dike breaches. Polder 48 in the coastal region, also known as Kuakata, was selected as the study area. A HEC-RAS 1D-2D inundation model was developed to simulate inundation under different scenarios. Tidal variations, angle of the cyclone at landfall, different dike breach locations, geometrical properties of the breach, breach propagation time and the sea level rise due to climate change according to the fifth assessment report (AR5) of Intergovernmental Panel on Climate Change (IPCC) were combined to develop the scenarios. The critical location of the dike breach was identified by comparing the three worst cases of the developed scenarios. Generated flood risk maps corresponding to the breaching at the critical location indicated that settlements adjacent to the canals face higher risk. The probabilistic flood map (PFM) calculated from the results of all the developed scenarios indicated the need of appropriate land use zoning to minimize the vulnerability to flooding. The developed model can be applied to generate location based flood forecasting, to identify critical locations of the dike to reduce the risk from flooding and to study the effect of climate change.

Bangladesh, one of the most disaster-prone countries, has a dynamic delta with 123 polders. Cyclone induced storm surges cause severe damages to these polders. This paper presents an investigation of the inundation pattern inside a polder due to dike failure caused by storm surges and identifies possible critical locations of dike breaches. Moreover risk of flooding was assessed and probabilistic flood map was generated due to breaching of dike to assist land use planning to increase preparedness

## 1. Introduction

Bangladesh is the low lying delta of three major rivers: Ganges, Brahmaputra and Meghna. Eighty percent of the country's land is located below 10m AMSL (above mean sea level) (Heitzman and Worden, 1989) and it is formed of sediments



carried by the above mentioned rivers. The population of Bangladesh is about 160 million (BBS, 2012) of which about 49% live in the coastal zones (Neumann *et al.*, 2015). The coastal areas of Bangladesh are flooded frequently due to cyclone induced storm surges and occasionally due to heavy rainfall in the upstream catchments of Ganges, Brahmaputra and Meghna. The coast was hit by 5 severe cyclones from 1995 to 2010 causing flooding, huge damages and loss of life (Dasgupta *et al.*, 2014).

Bangladesh has 123 polders in the coastal area surrounded by earthen dikes, designed to protect the land from flooding due to diurnal high tide. The existing crest level of these dikes are only adequate enough to protect the coastal area from cyclones with 5 to 12 year return periods (Islam *et al.*, 2013). These dikes usually get damaged by tropical cyclones of high intensity due to overtopping and scouring in the landside, which causes flooding inside the protected areas, damaging properties and causing loss of life. For example, cyclone Sidr hit the coast of Bangladesh in 2007 affecting 8.9 million people, causing US\$1.67 million of damage (GOB, 2008) and US\$70.3 million of damage to the dikes and control structures (Dasgupta *et al.*, 2014). In 2009, Cyclone Aila affected 3.9 million people with an estimated damage of US\$270 million (EMDAT, 2009). Crest levels of the coastal dikes were redesigned recently for an event of 25 year return period under the Coastal Embankment Improvement Project (CEIP) (BWDB, 2013). Raising the crest level was only considered as mitigating measure. Previous studies on the coastal areas of Bangladesh considered flooding only due to overtopping of the dikes. Effect of breaching of the dikes due to piping and scouring on the landside during cyclones have not been studied. Moreover, non-structural flood mitigation measures such as land use zoning using the flood risk map (FRM) and probabilistic flood map (PFM) to locate the vulnerable areas is currently unavailable for the coastal areas of Bangladesh.

Moreover, the intensity and frequency of these tropical cyclones will increase in the future due to climate change causing more damages. It is projected that by the year 2100, the frequency of the most intense cyclones will increase substantially and the intensity of tropical cyclones will increase by 2 to 11% due to global warming (Knutson *et al.*, 2010). Damage due to tropical cyclone will increase by US\$53 billion per year by the year 2100 due to climate change which is almost twice the damage without the effect of climate change (Mendelsohn *et al.*, 2012). Furthermore, flooding by tropical cyclones will increase in the future as a result of sea level rise (SLR) (Woodruff *et al.*, 2013). Countries situated at lower latitudes are predicted to suffer most from climate change (Mendelsohn *et al.*, 2006). Hence Bangladesh with the latitude of  $20.67^{\circ}$  N to  $26.58^{\circ}$  N may face severe consequences, and is predicted to be one of the most affected countries due to climate change (World Bank, 2015).

This paper presents a methodology to investigate the inundation pattern behind the dike and produce FRM and PFM due to breaching during a cyclone induced storm surge using a 1D-2D coupled model. The variation of storm surge height due to tidal conditions (diurnal, semi-diurnal and seasonal) and angle of cyclone at landfall along with different breach geometry (width, height and propagation) and different breach locations were considered in developing the scenarios. Analysis of the results of different scenarios led to the identification of critical locations of dike breaching.



## 2. Study area

Polder 48, which was considered as the study area for this research, is surrounded by dikes and has a sea facing dike of about 20 km length on the southern side of the polder. The polder is located in the south west coast of Bangladesh Delta (Figure 1) stretching from 21°50'28" N 90°05'17" E to 21°50'06" N 90°14'14" E. The area is also known as Kuakata and it is in the administrative zone of Kalapara sub-district of Patuakhali District. It has an area of 50.75 km<sup>2</sup> with 24,240 inhabitants according to the census of 2011. Most of the inhabitants are farmers and fishermen (Nasreen et al., 2013). Shrimp culture and tourism are also part of the economic activities. The land use is mainly classified into the following four classes: rice fields, settlements, shrimp ponds and water bodies (river/canal). Climate of Kuakata is similar to the climate of the country (Bangladesh). The average yearly rainfall in Kuakata is 2590mm (Climate-Data, 2016). The month with highest rainfall is July with an average of 611mm. The annual average temperature of Kuakata is 25.9°C with minimum and maximum temperature as 13°C and 34°C respectively (Climate-Data, 2016). There are three seasons for growing crops (DAE, 2009). They are, Rabi (November to February), Kharif-I (March to May) and Kharif-II (June to October). The area is relatively flat and low lying, with 80% of its elevation below 1.55m PWD, the vertical datum established by Public Works Department of Bangladesh, which is 0.46m above the MSL. The land level surveys at different times have indicated that this polder is facing land subsidence issues.

The area was severely affected by recent storms Sidr, Aila and Mohasen in 2007, 2009 and 2013 respectively. For example, during cyclone Sidr, 94 people died and 45% of the crops were lost in Kalapara sub-district (Ahamed, 2012).

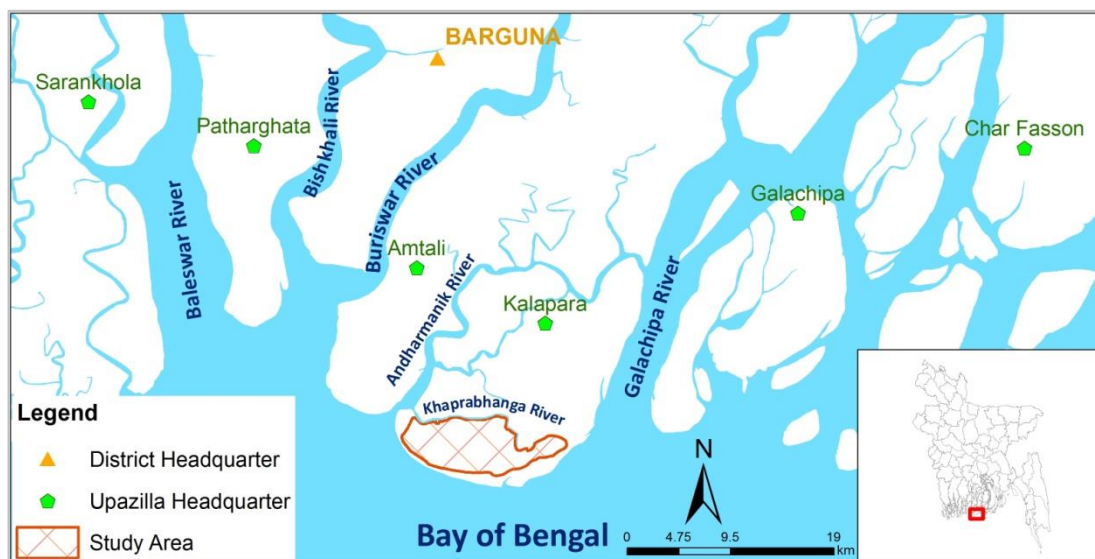


Figure 1: Location map of the study area Polder 48 (Kuakata).

Andharmanik, Galachipa and Khaprabhanga rivers are on the east, west and north of the study area respectively, whereas the Bay of Bengal is on the southern side of the study area (Figure 1). Galachipa River is the widest among the rivers surrounding the area. On the southern side, the study area has sea shore of 20 km width, which is protected by the mangrove



forest in several locations. There is a narrow sea beach in the south-western side of the area. The western part of the sea facing dike was overtopped during cyclone Sidr causing flood inside the polder (Hasegawa, 2008). The loss of livestock and food grains were such that it created partial deficiency of food in Kuakata (TANGO International, 2010). The average crest level of Polder 48 in the northern side is 4.5m PWD and in southern side (sea facing side) is 6m PWD at present (Islam *et al.*, 2013). The existing embankments of 17 polders, including Polder 48, were redesigned and rehabilitated during the first phase of CEIP (Islam *et al.*, 2013). CEIP proposed a crest level of 7.36m PWD for the dike of Polder 48 (Islam *et al.*, 2013).

### 3. Methodology

A 1D-2D hydraulic model was developed to simulate inundation corresponding to different scenario, which were formed by considering varying storm surges and breach location, and climate change. The inundation pattern consequent to dike breaching was analysed, tangible damages were estimated and flood risk maps were developed. A probabilistic flood map was generated using the result of all the simulated scenario.

#### 3.1 1D-2D model development

A 1D-2D inundation model was developed for the study area. Field measurements (land level survey, observed water level, canal alignment, cross sections of the rivers and canals etc.) and information from remote sensing (satellite imagery) were gathered for developing the model (Figure 2). Institute of Water Modelling (IWM) of Bangladesh carried out the feasibility study of Coastal Embankment Improvement Project (CEIP) and collected hydraulic, hydrologic and land level data for the polders. IWM has kindly provided the measured data. A 1D model was developed and calibrated using the information shared by IWM. The model was simulated using discharge as the upstream boundary and water level as the downstream boundary conditions. The calibrated 1D model was coupled with a Digital Elevation Model (DEM) to include the 2D component and overland flow. The DEM was generated from the land level survey conducted by IWM and FINMAP. The land level survey of IWM did not cover the whole study area. The gaps in land level survey of IWM were filled in with the data from a previous survey conducted by FINMAP, which was provided by IWM. FINMAP (a company from Finland) conducted the topographic surveys in 2000. The elevation differences of land survey of IWM (conducted in 2012) and FINMAP indicated the land subsidence. The FINMAP data was corrected for land subsidence using the arithmetic average of the differences of these two land level surveys for Polder 48. The combined DEM has a resolution of 50m.

For the 1D-2D inundation model, a computational mesh with a resolution of 50m was used. The roughness coefficient (Manning's  $n$ ) was provided according to the landuse of each cell. A sensitivity analysis as suggested by Hall *et al.* (2005) was carried out by varying Manning's roughness coefficient  $n$  before the calibration of the 2D inundation model. The analysis indicated that the inundation model is not highly sensitive to the roughness coefficient and the location furthest from the dike breach is most sensitive. The sensitivity analysis was done for the breaching on the western part of the dike only. It



was considered that the breaching at other locations will have similar effect as the area inside the polder is flat and low lying with mostly farmlands near the dike.

The bathymetric data for the sea was collected from global bathymetric chart of ocean (GEBCO) (Smith and Sandwell, 1997). The land use data was collected from the Ministry of Land of Bangladesh. MODIS reflectance data was used for the analysis of previous flood events. The methodology and equations suggested by Hoque *et al.* (2007) were used to analyse the MODIS reflectance data to determine flood extents during previous flood events.

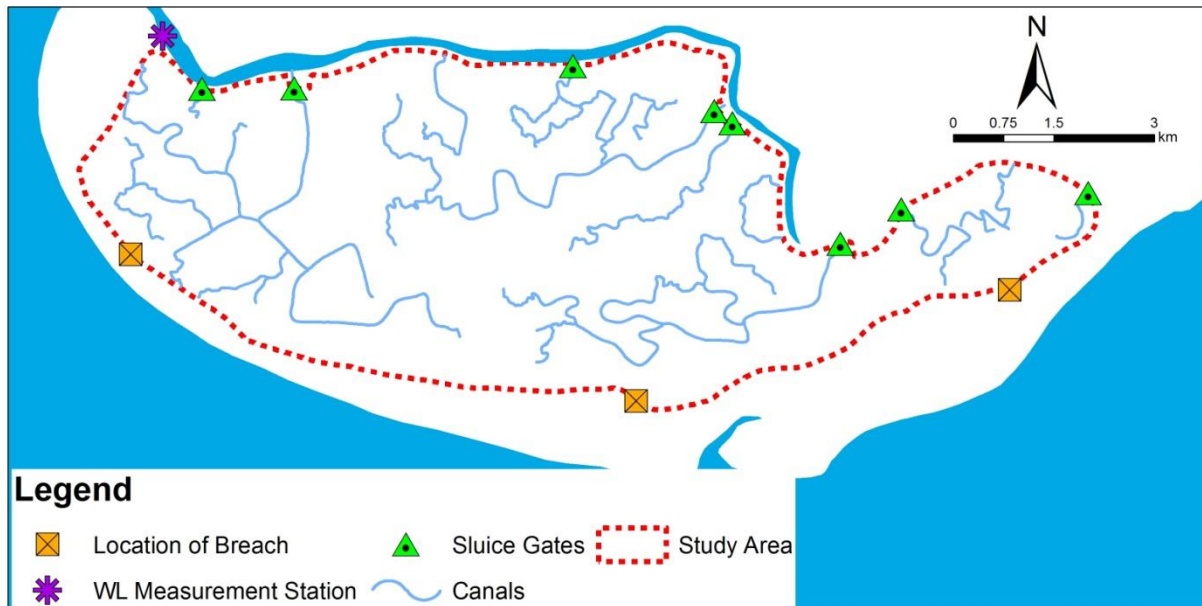


**Figure 2: Schematic diagram of the study area with location of control structures and gauges and the considered breach locations.**

The river analysis tool HEC-RAS from the US Army Corps of Engineers was used to develop the 1D-2D inundation model. Building and calibrating the 1D model was the preliminary step for developing the 1D-2D coupled model. The water bodies surrounding the study area were included in the 1D model. The study area has Khaprabhanga River on the northern side and sea on the southern side. For the rivers, the surveyed cross sections were used in the 1D model. To represent the sea and the storm surges, a 1D channel was added using the bathymetric data from GEBCO. The dense canal network of 122 km, inside the study area, is connected with the Khaprabhanga River, which regulates the in-and out flow into the network through a system of 13 control structures. The regulators remain closed during a cyclone making the canal network isolated. Therefore, the canal network inside the polder was not included in the 1D model. In order to ensure model stability a maximum spacing between the cross section was imposed and computed using Samuels' formula (1989) presented in Eq. (1):

$$\Delta x \leq 0.15 * D/S_0 \quad (1)$$

where,  $\Delta x$  is the spacing between cross-sections,  $D$  is the average bank full depth of the channel and  $S_0$  is the average slope of the channel. The maximum spacing between cross sections was calculated as 300 m.





As suggested by Fromm (1961) the Courant number was kept less than or equal to 1.0 to maintain the stability of the numerical model by controlling the time step. The Courant number was calculated using the following Eq. (2):

$$Cr = V * \Delta t / \Delta x \quad (2)$$

where  $Cr$  is Courant number,  $V$  is velocity,  $\Delta t$  is the time step and  $\Delta x$  is the spacing between the cross sections.

### 5 3.2 Cyclonic scenarios considered

Different scenarios were developed considering the probability of occurrence of cyclones, the angle of landfall, SLR due to climate change, diurnal, semi-diurnal and seasonal variation of tides, location of breaching of dike and geometrical properties of the breach. A cyclone of 1 in 25 year return period was considered for scenario development as this is used as the design criteria for the dikes (BWDB, 2013). Nineteen previous cyclones for different tidal conditions were simulated by IWM using a 2D model for the Bay of Bengal. A statistical analysis was conducted using these model results to generate the storm surge height corresponding to a cyclone of 25 year return period (Islam *et al.*, 2013). The angle of landfall and the tidal phase affect the height of storm surges. The storm surge height increases with angle of the storm to the coastline (Azam *et al.*, 2004). Angle of attack governs the wind speed which is one of the parameters for the height of cyclone induced storm surges (Azam *et al.*, 2013). The difference between the storm surge at high tide and low tide is 1.2m for the study area (Azam *et al.*, 2004). The average seasonal variation of the tidal range is 1.3m.

The coast of Bangladesh may be severely affected by SLR and one fourth of the land may be lost due to SLR by 2100, which will directly affect 3 million people (Ericson *et al.*, 2005). The land subsidence in the delta will exacerbate the effect of SLR. SLR and sea surface temperature (SST) will affect the cyclone induced storm surge height in the Bay of Bengal (Karim and Mimura, 2008). With increasing SST, the storm surge height can increase from 21% to 49% (Karim and Mimura, 2008) and with SLR, the flood depth due to storm surges may increase by 30-40% (Karim and Mimura, 2008). The Intergovernmental Panel on Climate Change (IPCC) published their 5th assessment report (AR5) in 2013. Among the scenarios considered in AR5, RCP (representative concentration pathways) 2.6 is the most optimistic one and RCP 8.5 is the worst considering the carbon emission, rise in temperature and SLR. The mean SLR at the end of 21st century is predicted to be 0.4m, 0.47m, 0.48m and 0.63m for scenario RCP 2.6, RC 4.5, RCP 6.0 and RCO 8.5 respectively (Stocker *et al.*, 2013). For this study, the worst case scenario RCP 8.5 with SLR of 0.63 m was considered for developing the scenarios.

The sections of the sea facing dike of the study area protected by mangrove forest, sand dunes and wide beach are least likely to be breached due to storm surges. The study considered breach locations with least protection. The considered locations are shown in Figure 2.

The geometry and propagation of the breach of the dike depends primarily on the storm surge height, angle of landfall, soil properties and wave action. The coastal embankments of Bangladesh are usually earthen embankments. The geometrical properties of the breaching of the dike and the time required for breaching were calculated following the instructions of US Bureau of Reclamation. An S-curve was used for breach propagation with time (Oumeraci, 2006).



For the generation of the probabilistic flood map (PFM), a scenario matrix consisting of 72 scenarios were generated combining different values of tidal level, angle of landfall, SLR and breach locations (Table 1). Single breach was considered for each scenario. The highest storm surge height among all the developed scenario was 7.2mPWD considering the SLR, worst angle of landfall and high tides, simultaneously. Due to the worst case of all the parameters, this storm surge height was considered for worst case scenarios. Breaching at west, central and eastern part of the dike with the highest storm surge were considered as the worst case scenarios and were denoted as Scenario 1, 2 and 3 respectively.

**Table 1: Storm surge heights corresponding to different scenarios considered.**

Angle of Landfall	Tidal Variation	Breach Locations						
		East		West		Central		
		With SLR	Without SLR	With SLR	Without SLR	With SLR	Without SLR	
Storm Surge Heights								
200	High Tide	Spring tide	4.06	3.38	4.06	3.38	4.06	3.38
		Neap tide	2.77	2.09	2.77	2.09	2.77	2.09
	Low Tide	Spring tide	2.83	2.15	2.83	2.15	2.83	2.15
		Neap tide	1.54	0.86	1.54	0.86	1.54	0.86
215	High Tide	Spring tide	6.16	5.48	6.16	5.48	6.16	5.48
		Neap tide	4.86	4.18	4.86	4.18	4.86	4.18
	Low Tide	Spring tide	4.93	4.25	4.93	4.25	4.93	4.25
		Neap tide	3.63	2.95	3.63	2.95	3.63	2.95
230	High Tide	Spring tide	7.20	6.52	7.20	6.52	7.20	6.52
		Neap tide	5.91	5.23	5.91	5.23	5.91	5.23
	Low Tide	Spring tide	5.97	5.29	5.97	5.29	5.97	5.29
		Neap tide	4.68	3.99	4.68	3.99	4.68	3.99

To identify the critical location for breaching of the dike results of the three worst case scenarios were compared using the total area flooded and estimated damage due to flooding. Using the calculated damage and occurrence probability of the event, a risk map was generated for the critical locations of the sea facing dike. A probabilistic flood map (PFM) was generated from the flood maps of the 72 scenarios (Table 1).

### 3.3 Estimation of damage due to floods

A comprehensive damage calculation should involve both direct and indirect damages due to floods (Büchle *et al.*, 2006). Direct damage is caused by physical contact of properties and human beings with flood water. Indirect damage is caused by interruption of services, production and transportation, degradation of health etc. due to floods. Due to lack of data, only the



direct damage to properties were calculated for the study area. The damage was considered as a function of depth. Depth-damage curves for different land classes for the study area were developed by adapting existing depth-damage curves from elsewhere (Figure 3). The land use of the study area was classified in residential areas (settlements), rice fields, shrimp ponds and rivers/canals by the Ministry of Land of Bangladesh. Only tangible damage was considered and no environmental damage was calculated. Damages to the canal network was not considered. The damage in a flood event was calculated using the following Eq. (3).

$$D = \left( \sum_{i=0}^n x_i \times f(x_i) \right) \times A_i \quad (3)$$

Where,  $D$  = total direct tangible damage,  $n$  = total number of computational cells within the flooded area,  $x$  = flood depth of cell  $i$ ,  $f(x)$  = damage function for the land use of the flooded cell  $i$  and  $A_i$  = area of cell  $i$ .

Reese *et al.* (2010) calculated flood damage as a percentage of the value of the property for different building types according to the construction material. The buildings of the study area are primarily built of timber due to its low cost and easy availability. The depth-damage ratio curve suggested by Reese *et al.* (2010) for buildings made of timber was used for generating the depth-damage curve for the settlements (residential area). Simple Action for the Environment (SAFE) carried out a research on the average value of properties in rural areas of Bangladesh (SAFE, 2011). This property values were used to develop the depth-damage curve for the settlements of the study area. As the rural houses in Bangladesh usually have a lot of open and unoccupied spaces, 50% of the area of a settlement was considered areas with no damages.

The cultivation of rice involves flooding the rice field with water of several cm. But if the height of water increases and the rice plant goes under water, the productivity decreases. The damage to rice plants also depends on the flood duration. If the rice plant is continuously under water for more than 2-3 days then the damage can be up to 80% (Chau *et al.*, 2014). The depth-damage curve suggested by Chau *et al.* (2014) was used for the study area.

Based on the practices in the study area the banks of the shrimp ponds were considered as 2 meter above the adjacent land. Therefore, it was assumed that there will be no damage shrimp ponds till the flood depth reaches 2 meter. However, after the flood level goes above the banks of the shrimp ponds the shrimp will escape to the flooded area and cause a loss of the total investment. To take this into account, the investment made by farmers was assessed using a study conducted by Fatema *et al.* (2011). According to the study the investment for shrimp pond in the study area was about 0.09 Euros per square meter.



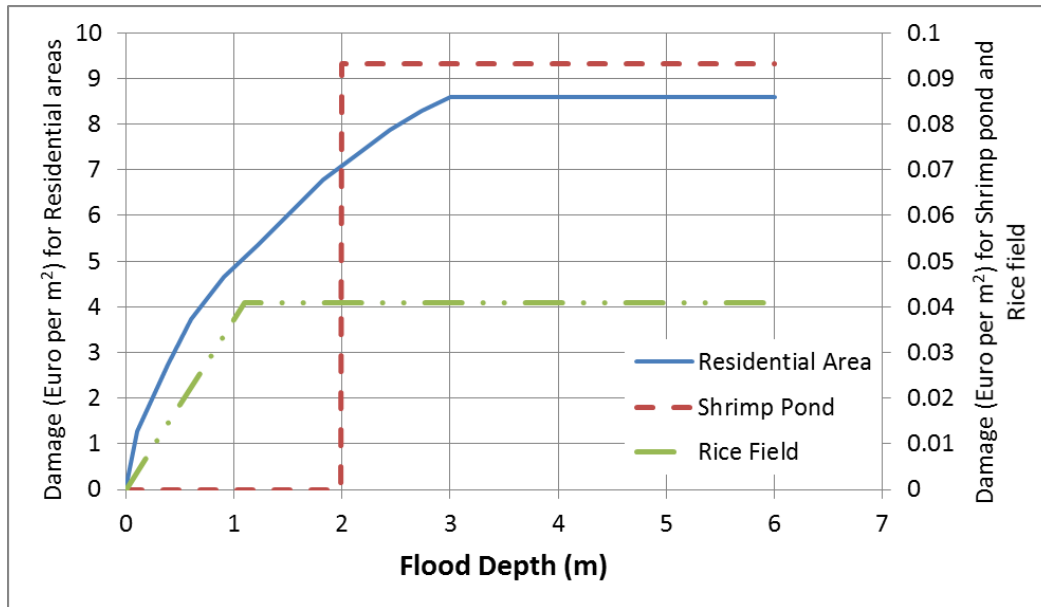


**Figure 3: Depth-damage curves for different land use classes.**

For carrying out damage calculations, a simple tool was developed in ArcGIS. The tool uses simulated inundation map and landuse map as the input, calculates damage in grid cells by identifying landuse class and flood depth, and by applying the appropriate depth-damage curve. The damage for each scenario was estimated using this tool. The critical location of breaching was selected by considering maximum flooded area and estimated flood damage. The developed depth-damage curve obviously is a simple one, which was built by updating the existing ones. More research is needed to improve the depth-damage curve.

### 3.4 Calculation of flood risk and generation of risk map

Flood risk assessment is an essential part of risk management. Spatial distribution of risk and areas requiring mitigation measures can be identified from flood risk maps (Meyer *et al.*, 2009). To examine the spatial variation of risk, flood risk analysis was carried out and a risk map was generated considering dike breaching at the critical location. Van Manen and Brinkhuis (2005) and Klijn (2009) under FLOODsite project carried out research to quantify the flood risk for the polders in The Netherlands for dike failure defining the risk as a product of the occurrence probability of the event and the consequences. The following Eq. (4) developed from FLOODsite definition was used to calculate the risk due to flooding:

$$R = P_F * S \tag{4}$$

Where,  $R$  = risk,  $P_F$  = probability of occurrence of the flood hazard and  $S$  = consequences

The exceedance probability (return period) of the cyclone induced storm surge was used as the probability of occurrence of the hazard. The probability of flooding within a protected area is not the same as the probability of the hazard and depends also upon the probability of failure of the dike. It is a difficult probability to compute as the probability of dike failure also



depends upon the dike maintenance and we did not have information about dike maintenance. As a simplistic approach here we have assumed that the probability of occurrence of the hazard and the probability of failure of dike as the same.

### 3.5 Probabilistic flood map

Purvis *et al.* (2008) stated that the risk assessment for the most probable scenario cannot take into account the impact of  
5 scenario of low probability stressing the necessity of a probabilistic risk analysis. The equation used by Purvis *et al.* (2008) was adjusted for this research to calculate the probability of flooding of each cell and is presented below in Eq. (5):

$$P_i = \frac{\sum_j F_{ij} \times P_{fj}}{\sum_j P_{fj}} \text{ and } F_{ij} = \begin{cases} 1, & \text{if flooded} \\ 0, & \text{if dry} \end{cases} \quad (5)$$

Where,  $P_i$  is probability of flooding at cell  $i$ ,  $P_{fj}$  is the probability of reaching a certain storm surge level in simulation  
10 number  $j$ ,  $F_{ij}$  is the binary value indicating if the cell  $i$  is flooded or not in simulation  $j$ ,  $j = 1, 2, 3, \dots, M$  where  $M$  is the number of scenarios considered ( $=72$ ),  $i = 1, 2, 3, \dots, N$  are the computational grid cells on the polder area and  $N$  is the number of cells. Equation (5) was used in this paper to calculate the probability of flooding at each cell. The probabilistic flood map (PFM) was calculated using the results of all the scenarios of the developed scenario matrix.

## 4. Results and discussion

A 1D-2D model was developed and simulated for different scenarios in this study. The 1D part of the model was calibrated  
15 by comparing the observed and simulated water level and discharge. The coefficient of determination ( $R^2$ ), root mean square error (RMSE) and mean absolute error (MAE) were 0.98, 2.15 m<sup>3</sup>/s and 1.68 m<sup>3</sup>/s respectively for discharge and 0.98, 0.09 m and 0.08 m respectively for water level. The average discharge and water level was 5.68 m<sup>3</sup>/s and 0.82 m respectively for the simulation period. The calibrated model was simulated for the storm surges corresponding to cyclone Sidr (from November 14 to November 17, 2007). The simulation results indicated that the sea facing dike of the study area was  
20 overtopped and the area inside the polder was inundated. The survey conducted by Japan Society of Civil Engineers (JSCE) after cyclone Sidr had similar findings (Hasegawa, 2008).

No flood maps showing flood extents for recent cyclones were available for the study area to calibrate the 1D-2D model. MODIS reflectance data was analysed for inundation. The availability of MODIS data was challenged due to the cloud  
25 coverage during the cyclones. The survey conducted by JSCE after cyclone Sidr was collected to investigate the flood extent and depth. Flood depth for only one location inside the study area was provided by JSCE. This location was used for the calibration of 2D model. The error in the simulated flood depth was 4.5%.

The 1D-2D model, with limited calibration, was used in simulating the developed scenarios. The simulated results were used in analysing flood depth, flood extent and damages due to flood. The FRM and the PFM were generated from the results.



#### 4.1 Inundation corresponding to three worst case scenarios

Among the simulated scenarios, the results of three worst case scenarios (Scenario 1, 2 and 3) were compared for identifying the critical location of breaching. The flood maps were created from the simulated results. The flood maps for the worst case scenarios are presented in Figure 4.



**Figure 4:** Flood extent corresponding to three worst case scenarios of dike breaching in the central, eastern and western section of the dike.

- 5 Flood extents corresponding to all different scenarios presented in Table 1 were compared to understand the effect of SLR, diurnal and seasonal tidal variation and angle of cyclone at landfall. The flood extends of different scenarios considering the breaching at central part of the sea facing dike is presented in Fig. 5.

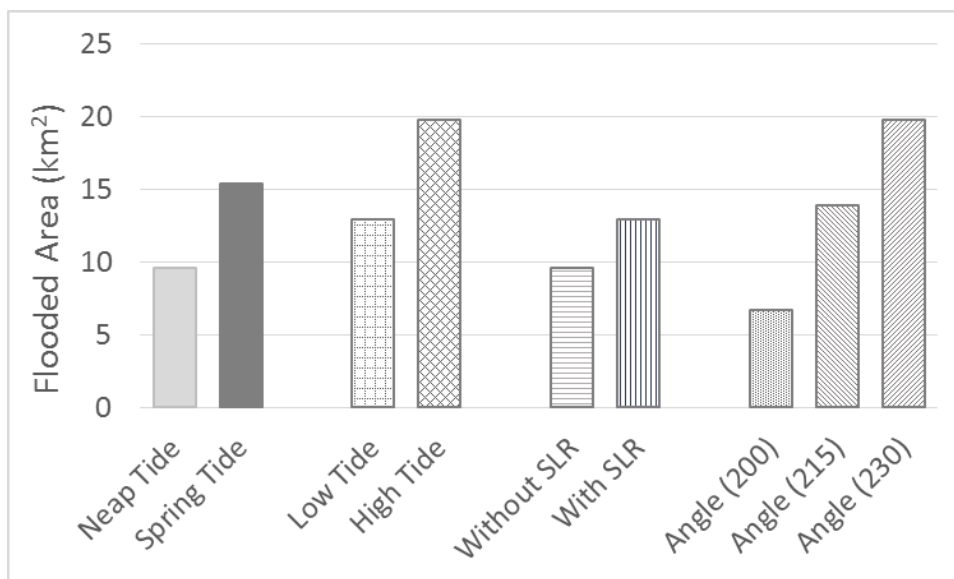


**Figure 5: Comparison of flooded areas corresponding to different scenarios.**

The flooded areas for different land classes were calculated for the three worst case scenarios (Table 2 **Error! Reference source not found.**). The flooded areas for different flood depth ranges were also analysed (Figure 6).

**Table 2: Flooded areas of different land classes corresponding to the three worst case scenarios.**

Land Classes	Flooded Area (km <sup>2</sup> )		
	Scenario 1	Scenario 2	Scenario3
Rice Fields	15.3	16.4	12.3
Settlements	3.1	3.1	2.1
Shrimp Ponds	0.2	0.1	0.1
Canals	1.2	1.7	1.2
Total	19.8	21.2	15.8

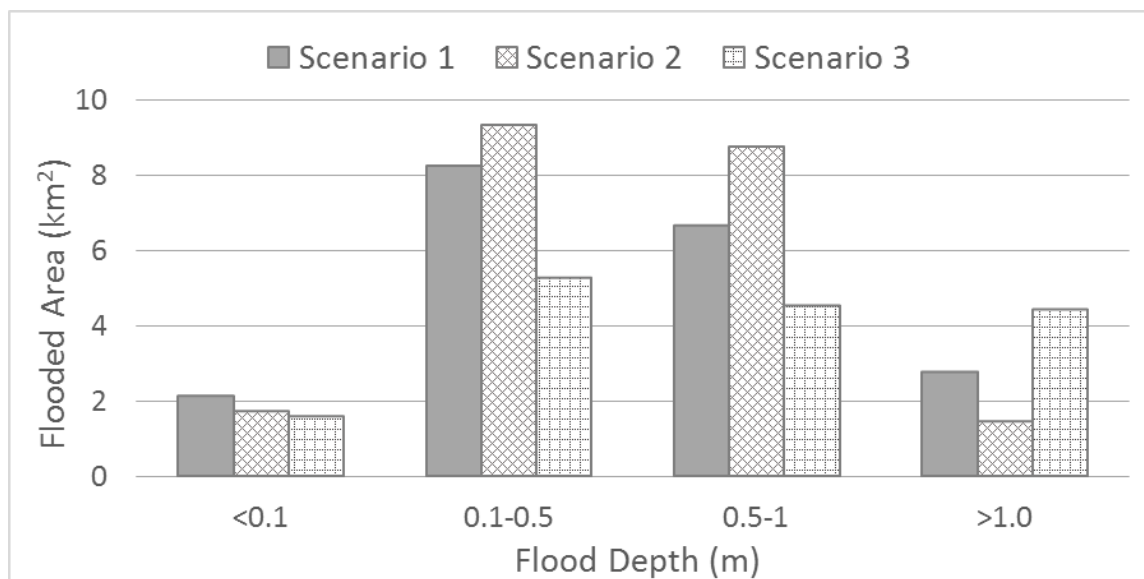


Figure 6: Flooded areas for different ranges of flood depths corresponding to different scenarios.

#### 4.2 Comparison of calculated damages

The damage due to flooding was calculated using the depth-damage curves for different land classes (Fig 3) and the tool developed in ArcGIS. The calculated damages for different land classes and damages for different flood depths corresponding to the three worst case scenarios are presented in Table 3 and Figure 7.

5

Table 3: Calculated flood damages for different land classes corresponding to different scenarios.

Land Classes	Estimated flood damage (million Euros)		
	Scenario 1	Scenario 2	Scenario 3
Rice Fields	0.4	0.4	0.3
Settlements	10.3	10.3	8.3
Shrimp Ponds	0.0	0.0	0.0
Total	10.7	10.7	8.7

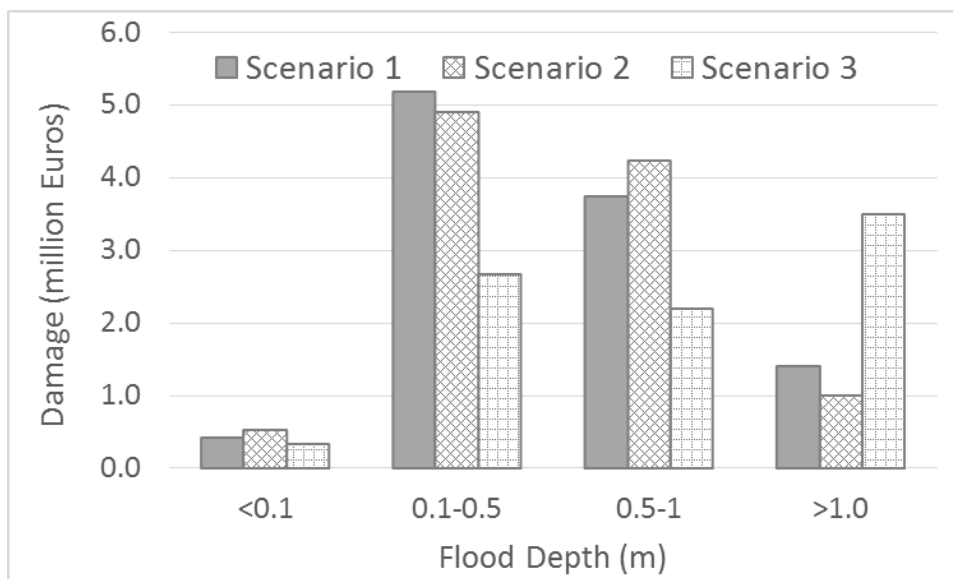


**Figure 7: Variation of estimated flood damages with varying ranges of flood depths corresponding to Scenario 1, 2 and 3.**

#### 4.3 Risk map for the worst case scenario

The flood risk map for the scenario with critical location of breaching of dike is presented in Figure 8. The risk maps were generated using the process explained in the previous section (Methodology). The risk map presents the assessed risk of flooding due to breaching at critical locations of the dike. The identification of the critical location of breaching is described

5 in the following section.



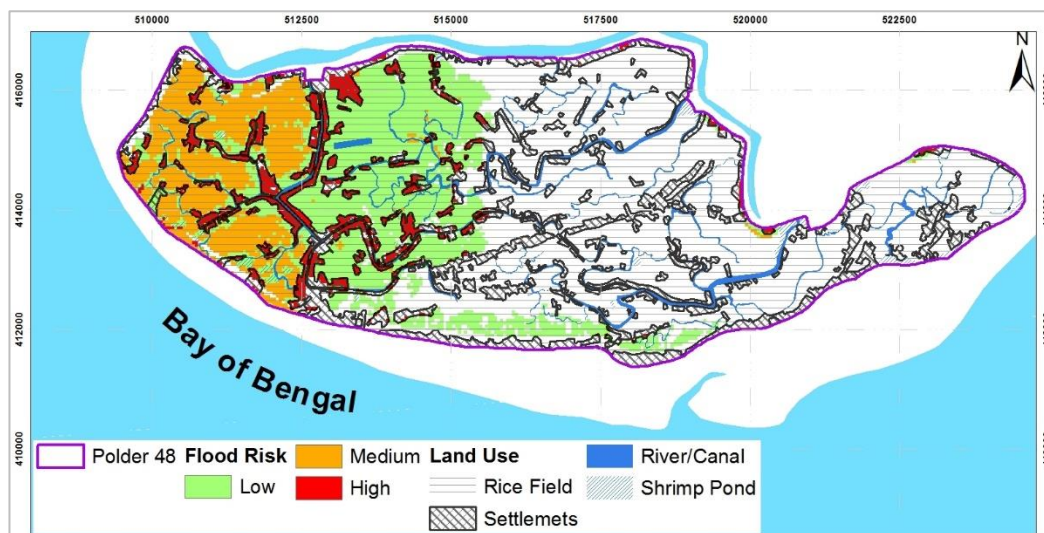


**Figure 8:** Flood risk map corresponding to the dike breach at the critical location of the dike. The following three classes of risk are shown: high, medium and low. The considered four landuses are shown as well.

#### 4.5 Probabilistic flood map

Although the inundation maps are widely used for spatial planning and flood mitigation measures, the uncertainty of mathematical modelling tool affects the output of inundation maps (Alfonso *et al.*, 2016). To take the uncertainty into account, probabilistic flood maps are used (Domeneghetti *et al.*, 2013). The probabilistic flood map was calculated from the inundation maps corresponding to the 72 scenarios considered in the study. Probabilistic flood maps were calculated for a threshold of flood depth greater than 0.5m. The calculated probabilistic flood maps are presented in Figure 9. The probabilistic flood map indicates the likelihood of being flooded. This will assist the planning for future land use zoning to restrict development in the floodplains.

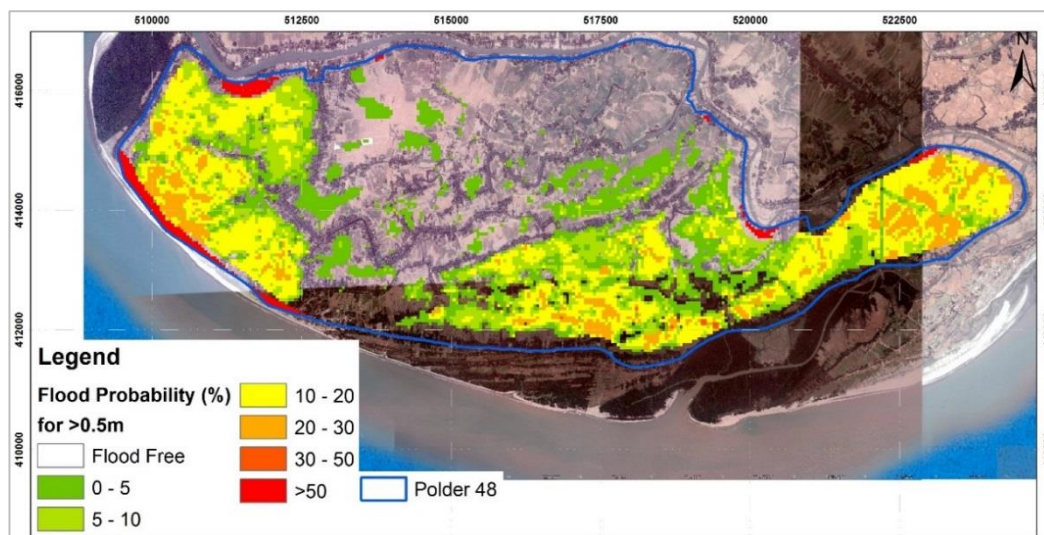


**Figure 9: Probabilistic flood map of the study area. Varying colours indicate probabilities of obtaining flood depths more than 0.5m.**

#### 4.6 Discussion on the results

Among the scenarios developed, the results of three worst case scenarios (Scenario 1, 2 and 3) were compared by generating flood maps, calculating total flooded areas and total damages. The flood maps for Scenario 1, 2 and 3 (Figure 4) demonstrate that the depth of flooding gradually decreases as the water moves inland. More than 25% of the total area of Polder 48 was inundated for all the three worst case scenarios (Table 2 **Error! Reference source not found.**). With all 3 scenarios the inundation area with flood depths 0.5 to 1.0 m was larger than the inundation areas with other flood depths (Figure 6). The inundation area with flood depths more than 1m was largest for Scenario 3 due to the depressions close to the dikes (Figure 6). The rice fields were flooded most and shrimp ponds were flooded least for all the scenarios (Table 2).

The total estimated damages due to flooding for Scenario 1, 2 and 3 were 10.71, 10.67 and 8.61 million Euros (Table 3). The damage to the settlements was greater than other land classes for all the scenarios (Table 3). Rice fields were flooded most but they did not experience the highest damage compared to other landuse classes (**Error! Reference source not found.** Table 2 and Table 3). This can be explained by the high damages in settlements compared to rice fields (Fig. 3). The damage to crops depends on the flood depth, duration and overland flow velocity. For simplification, only the damage related to flood depth was used. The primary economic activity of the inhabitants of the study area is farming and most of the inhabitants are poor. Even though the damage to crops are much less compared to other land uses, it will affect the people living in the study area most as they depend on the farming of rice for their livelihood (Nasreen *et al.*, 2013). Hasan *et al.* (2004) found out that the dependence on fishing (in the sea) by the inhabitants of Polder 48 are increasing due to loss of crops by flood, loss of productivity, lack of jobs and poverty. Fishing in the sea is a risky profession for the coastal region of Bangladesh as it yields lower economic returns leading to enhanced poverty (Hasan *et al.*, 2004).



The damage was maximum with flood depths 0.1 to 0.5m for all the scenarios (Figure 7). The damage due to inundation less than 0.1m was small and insignificant. The estimated flood damage increased significantly for inundation more than 0.5m. The threshold for calculating probabilistic flood maps (PFM) was set to 0.5m of flood depth, as the estimated flood damage increased for flooding more than 0.5m. PFM with the threshold of 0.5m identified the areas at risk of higher damage due to flooding.

Damage due to flooding was maximum for Scenario 1. Flooded area for settlements of Scenario 1 was lower than Scenario 2 (Table 2) but the estimated damage for settlements of Scenario 1 was more than Scenario 2 (Table 3). This indicates that the settlements for scenario 1 were exposed to greater flood depth than scenario 2. Furthermore, the total flooded area was higher for scenario 2 than scenario 1, but the estimated total damage was higher for scenario 1 (Fig. 6 and Fig. 7). Considering these facts, scenario 1 was selected as the worst case scenario and breaching at the western part of the sea facing dike was identified as the critical location for breaching during cyclone.

The probability of occurrence of the storm surge and damage caused by inundation were taken into account consideration for the risk calculation. In case of breaching of the dike, the probability of flooding was considered the same as the probability of occurrence of storm surge. The depicted risk map (Fig. 8) shows the areas adjacent to the dike breach is at higher risk and the risk reduces as the flood propagates towards east.

Canals are used as a mode of transportation by the inhabitants of the area. Most of the economic activities and residential areas are by the canals. The risk analysis show that the areas at highest risk are the residential areas (settlements) by the canals (Fig. 8). Therefore, although canals plays a crucial role in the economy and social life of the area, they also increase the risk of flooding.

Land use plan plays an important role in reduction of vulnerability to disasters (Burby, 1998). Probabilistic flood maps (PFM) can be used for land use planning (Alfonso *et al.*, 2016). For better understanding of the area at risk of flooding due to breaching of dike, probabilistic flood maps (PFM) were generated for the study area (Fig. 8 and Fig. 9). The results of 72 scenarios from scenario matrix was used for calculation of PFM. The areas adjacent to the sea dikes had higher probability of flooding due to breaching of dike for both PFMs. The areas inland had lower probability of flooding. Existing land use indicates that the areas with lower probability of flooding are mostly rice fields (Fig. 8 and Fig. 9). Land use zoning and management using the PMF can reduce the vulnerably and if used properly can lead to economic growth.

## 5. Conclusions

A 1D-2D coupled model was developed to investigate inundation pattern behind the dike due to breaching by cyclone induced storm surges. Different scenarios were developed and the results of these scenarios were compared using total flooded area and estimated damage.

Inundation for three worst case scenarios indicated that maximum flooded area occurs during the breaching of central part of the sea facing dike. Most flooded area had flood depth of 0.1 to 0.5 m for all three breaching locations witch scenario 2 with



breaching at the central part had the highest. Damage for scenario 1 (breaching at western part) and scenario 2 (breaching at central part) were equal, whereas scenario 1 had higher damage for flood depth of 0.1m to 0.5 m and scenario 2 had higher damage for flood depth of 0.5m to 1.0m. From these findings it can be concluded that the flood extents, flood depth and damage due to flood in case of breaching of the dike depends on breach location. Moreover, the comparison of the flood damages and flood extent led to identification of scenario 1 as the worst case scenario and western part of the sea facing dike as the critical location for breaching.

The generated flood risk maps indicated that for all the scenarios areas adjacent to the dike and canals inside the polder had higher risk. For better access to the canals for transportation and livelihood, development of infrastructure and households nearby the canals consequently increases vulnerability. Similarly, developing land for infrastructure and household on the country side of the dikes increases vulnerability. Combining effect of increased vulnerability and higher flood depth results in elevated risk of flooding due to dike breach during a cyclone.

Probabilistic flood maps generated by considering all the scenarios indicated that the rice fields and settlements are least and most probable land use respectively. Although the inhabitants are mostly dependent on agriculture, the flooding of settlements will cause most damage and forced relocation.

Measured storm surge level for previous cyclones were unavailable. Therefore, for this research synthetic water level time series were generated considering the storm surge height presented by Islam *et al.*, 2013, for a cyclone of 25 year return period. Furthermore, it was assumed that the cyclone will always cause breaching which resulted in storm surge and breaching having the same probability of occurrence.

Bangladesh is a hazard prone country and cyclone induced storm surge is one of many disasters experienced by the coast of Bangladesh. The storm surges case severe damage to the earthen embankment/dikes protecting the coastal polders and flood the area inside the coastal polders. The methodology presented in this paper to develop 1D-2D inundation model, PFM, risk maps and identify the critical location for breaching can assist in better preparedness by improved flood forecasting and flood risk and damage reduction by land use zoning and management. Flood forecasting and warning system using the developed coastal inundation model can provide valuable information to the farmers which could lead to early harvesting, construction of temporary barriers etc. Land use zoning using the risk maps and PFM can indicate the settlements, growing tourism and dry fish industry of the study area to safe or flood free zone for future development and relocation. The economic development and employment opportunity as results of will end the problem of poverty and provide hope of better life to the inhabitants.

## 6. Acknowledgements

The support of Institute of Water Modelling (IWM), Dhaka, Bangladesh, in providing the surveyed data is gratefully acknowledged.



## References

- Ahamed, S., Rahman, M.M. and Faisal, M.A.: Reducing Cyclone Impacts in the Coastal Areas of Bangladesh: A Case Study of Kalapara Upazila. *J. of Bangladesh Institute of Planners ISSN, 2075*, pp 9363, 2012.
- 5 Alfonso, L., Mukolwe, M.M. and Di Baldassarre, G.: Probabilistic Flood Maps To Support Decision- Making: Mapping the Value of Information. *Water Resources Research*, 52 (2), pp.1026-1043, 2016.
- Azam, M.H., Samad, M.A. and Mahboob-Ul-Kabir.: Effect of Cyclone Track And Landfall Angle on The Magnitude of Storm Surges Along the Coast of Bangladesh in the Northern Bay of Bengal. *Coastal Engineering J.*, 46(3), pp 269-10 290, 2004.
- Bangladesh Bureau of Statistics (BBS):. Population Census 2011. Available online at: [http://www.bbs.gov.bd/Census2011/Khulna/Khulna/Khulna\\_C01](http://www.bbs.gov.bd/Census2011/Khulna/Khulna/Khulna_C01) [Accessed 25 February 2016], 2012.
- Bangladesh Water Development Board (BWDB):. Technical Feasibility Studies and Detailed Design for Coastal 15 Embankment Improvement Programme (CEIP) (Main Report), Ministry of Water Resources, Government of the People's Republic of Bangladesh. Available online at: <http://bwdb.gov.bd/archive/pdf/364.pdf>, 2013.
- Burby, R.J. ed.: *Cooperating with Nature: Confronting Natural Hazards with Land-Use Planning for Sustainable Communities*. Joseph Henry Press, 1998.
- Büchle, B., Kreibich, H., Kron, A., Thieken, A., Ihringer, J., Oberle, P., Merz, B. and 20 Nestmann, F.: Flood-Risk Mapping: Contributions Towards an Enhanced Assessment of Extreme Events and Associated Risks. *Natural Hazards and Earth System Sciences*, 6(4), pp 485-503, 2006.
- Center for Research on the Epidemiology of Disaster. EMDAT- The International Disaster Database. [ONLINE] Available at: <http://www.emdat.be/database>. [Accessed 16 May 2016], 2009.
- 25 Chau, V.N., Cassells, S.M. and Holland, J.: Measuring Direct Losses to Rice Production From Extreme Flood Events in Quang Nam Province, Vietnam. In *2014 Conference (58th), February 4-7, 2014, Port Macquarie, Australia* (No. 165813). Australian Agricultural and Resource Economics Society, 2014.
- Climate-Data. *Climate: Kuakata*. Available online at: <http://en.climatedata.org/location/969757/> [Accessed 11 March 2016], 30 2016.
- Dasgupta, S., Huq, M., Khan, Z.H., Ahmed, M.M.Z., Mukherjee, N., Khan, M.F. and Pandey, K.: Cyclones in A Changing Climate: The Case of Bangladesh. *Climate and Development*, 6(2), pp 96-110, 2014.





- Domeneghetti, A., Vorogushyn, S., Castellarin, A., Merz, B. and Brath, A.: Probabilistic Flood Hazard Mapping: Effects of Uncertain Boundary Conditions. *Hydrology and Earth System Sc.*, 17(8), pp 3127-3140, 2013.
- Ericson, J.P., C.J. Vorosmarty, S.L. Dingman, L.G. Ward, and M. Meybeck.: Effective Sea-Level Rise and Deltas: Causes of Change and Human Dimension Implications. *Global Planetary Change* 50, pp 63-82, 2005.
- 5 Fatema, K., Miah, T.H., Mia, M. and Akteruzzaman, M.: Rice Versus Shrimp Farming in Khulna District of Bangladesh: Interpretations of Field-Level Data. *Bangladesh J. of Agri. Economics*, 34(1-2), 2011.
- Fromm, J.E.: Lagrangian Difference Approximations for Fluid Dynamics (No. LA-2535). Los Alamos National Lab Nm, 10 1961.
- Government of Bangladesh (GOB):. Damage, Loss and Needs Assessment for Disaster Recovery and Reconstruction, Cyclone Sidr, Bangladesh. Government of Bangladesh, pp 21, 27-28, 2008.
- Hall, J.W., Tarantola, S., Bates, P.D. and Horritt, M.S.: Distributed Sensitivity Analysis of Flood Inundation Model Calibration. *J. of Hyd. Engg*, 131(2), pp 117-126.
- 15 Harrington, B.W., 2005. Hazard Classification & Danger Reach Studies for Dams, 2005.
- Hasan, M., Billah, M.M. and Roy, T.K.: Tourism and Fishing Community of Kuakata: A Remote Coastal Area of Bangladesh, Part-1. *Support for University Fisheries Education and Research Project, Department for International Development, UK*, 2004.
- Hasegawa, K.: Features of Super Cyclone Sidr to Hit Bangladesh in Nov 07 and Measures for Disaster from Results of JSCE Investigation. In Proceedings of the WFEO-JFES-JSCE joint international symposium on disaster risk management. Sendai, Japan, 2008.
- 20 Heitzman, J. and Worden, R.L.: Bangladesh, A Country Study, Washington GPO (U.S. Government Publishing Office), 1989.
- Hoque, M.A.A., Phinn, S., Roelfsema, C. and Childs, I.: Assessing Tropical Cyclone Damage Using Moderate Spatial Resolution Satellite Imagery: Cyclone Sidr, Bangladesh, Proceedings of the 36th Asian Conference of Remote Sensing, 2007,
- 25 Islam, M., Khan, M., Alam, R., Khan, M. and Nur-A-Jahan, I.: *Adequacy Check of Existing Crest Level of Sea Facing Coastal Polders by the Extreme Value Analysis Method*. IOSR J. of Mechanical and Civil Engg., 8(1), pp 89-96, 2013,
- 30 Karim, M.F. and Mimura, N.: Impacts of Climate Change and Sea-Level Rise on Cyclonic Storm Surge Floods in Bangladesh. *Global Environmental Change*, 18(3), pp 490-500, 2008.
- Klijn, F.: Flood risk assessment and flood risk management; an introduction and guidance based on experiences and findings of FLOODsite (an EU-funded integrated project). Deltares, 2009.





- Knutson, T.R., McBride, J.L., Chan, J., Emanuel, K., Holland, G., Landsea, C., Held, I., Kossin, J.P., Srivastava, A.K. and Sugi, M.: Tropical Cyclones and Climate Change. *Nature Geoscience*, 3(3), p.157, 2010.
- Mendelsohn, R., Dinar, A. and Williams, L.: The Distributional Impact of Climate Change on Rich and Poor Countries. *Environment and Development Economics*, 11(2), pp 159-178, 2006.
- 5 Mendelsohn, R., Emanuel, K., Chonabayashi, S. and Bakkensen, L.: The Impact of Climate Change on Global Tropical Cyclone Damage. *Nature climate change*, 2(3), p.205, 2012.
- Meyer, V., Scheuer, S. and Haase, D.: A Multicriteria Approach for Flood Risk Mapping Exemplified at the Mulde River, Germany. *Natural hazards*, 48(1), pp 17-39, 2009.
- Nasreen, M. and Azad, M.A.K.: Climate Change and Livelihood in Bangladesh: Experiences of People Living in Coastal Regions. *Proc. of Int. Conf. on Building Resilience*, pp 1-25, 2013.
- 10 National Oceanic and Atmospheric Administration (NOAA): The Worst Natural Disasters by Death Toll. Available online at: [http://docs.lib.noaa.gov/noaa\\_documents/NOAA\\_related\\_docs/death\\_toll\\_natural\\_disaster.pdf](http://docs.lib.noaa.gov/noaa_documents/NOAA_related_docs/death_toll_natural_disaster.pdf) [Accessed 08 March 2016], 2008.
- Neumann, B., Vafeidis, A.T., Zimmermann, J. and Nicholls, R.J.: Future Coastal Population Growth and Exposure to Sea-Level Rise and Coastal Flooding-A Global Assessment. *PloS one*, 10(3), 2015.
- 15 Oumeraci, H., Breaching of Coastal Dikes: State of the Art. TU Braunschweig, 2006.
- Parry, M., Canziani, O. and Palutikof, J. eds.: Climate change 2007: impacts, adaptation and vulnerability (Vol. 4). Cambridge: Cambridge University Press, 2007.
- Purvis, M.J., Bates, P.D. and Hayes, C.M.: A Probabilistic Methodology to Estimate Future Coastal Flood Risk Due to Sea Level Rise. *Coastal engineering*, 55(12), pp 1062-1073, 2008.
- 20 Reese, S. and Ramsay, D.: RiskScape: Flood fragility methodology. *Wellington, New Zealand. National Institute of Water and Atmospheric Research*, p.42, 2010.
- Ritter, S.K., Global Warming and Climate Change. *Chem. Eng. News*, 12(21), pp.11-21, 2009.
- Samuels, P.G.: Backwater Lengths in Rivers. *Proc. of the Inst. of Civil Engineers*, 87(4), pp 571-582, 1989.
- 25 Sarwar, M.G.M.: Impacts of Sea Level Rise on the Coastal Zone of Bangladesh. Available online at: [http://static.weadapt.org/placemarks/files/225/golam\\_sarwar.pdf](http://static.weadapt.org/placemarks/files/225/golam_sarwar.pdf) (Accessed: 25th May, 2016), 2005.
- Simple Action for the Environment (SAFE), *Case Study: Construction of Improved Rural House in Dinajpur, Bangladesh*. Housing and Hazards: Simple Action for the Environment (SAFE), 2011.
- 30 Smith, W.H. and Sandwell, D.T.: Global sea floor topography from satellite altimetry and ship depth soundings. *Science*, 277(5334), pp 1956-1962, 1997.
- Stocker, T.F., Qin, D., Plattner, G.K., Tignor, M., Allen, S.K. and Boschung, J.: Climate Change 2013: The Physical Science Basis. Working Group 1 (WG1) Contribution to the



- Intergovernmental Panel on Climate Change (IPCC) 5th Assessment Report (AR5). Cambridge, United Kingdom and New York, NY, 2013.
- TANGO International.: *An Assessment of Livelihood Recovery*. DAP Emergency Program (Cyclone Sidr Response). Save the Children Bangladesh, 2010.
- 5 Van Manen, S.E. and Brinkhuis, M.: Quantitative Flood Risk Assessment for Polders. *Reliability engineering & system safety*, 90(2), pp 229-237, 2005.
- Woodruff, J.D., Irish, J.L. and Camargo, S.J.: Coastal Flooding by Tropical Cyclones and Sea-Level Rise. *Nature*, 504(7478), p.44, 2013.
- World Bank.: “Vulnerable Twenty” Ministers Call for More Action and Investment in Climate Resiliency and Low-Emissions Development. Available online at: <http://www.worldbank.org/en/news/feature/2015/10/08/vulnerable-twenty-ministers-moreaction-investment-climate-resilience-low-emissions-development>. [Accessed 22 February 16], 2015.
- 10